



## STUDIES ON THE NONLINEAR RESPONSES OF THE UNDERGROUND STRUCTURE SUBJECTED THE FAULT DISPLACEMENT

T. Sasaki<sup>(1)</sup>, S. Higuchi<sup>(1)</sup>, N. Watanabe<sup>(1)</sup>, K. Tanaka, K. Yonezawa<sup>(1)</sup>, T. Tsutsumiuchi<sup>(1)</sup>, H. Nagai<sup>(1)</sup>,  
K. Yamaguchi<sup>(2)</sup>, G. Itoh<sup>(2)</sup>, Y. Hida<sup>(2)</sup>

<sup>(1)</sup> Obayashi Co., [sasaki.tomohiro@obayashi.co.jp](mailto:sasaki.tomohiro@obayashi.co.jp)

<sup>(2)</sup> Tohoku Electric Power Co., [yamaguchi.kazuhide.ek@tohoku-epco.co.jp](mailto:yamaguchi.kazuhide.ek@tohoku-epco.co.jp)

### Abstract

Aim of this study is to evaluate the impact of the strike slip fault displacements against the RC underground structure. Firstly, centrifuge experiments were conducted to investigate the characteristics of earth pressure acting on the underground structure quantitatively during the fault movement. Then, numerical simulations were conducted to investigate the reproducibility of the external force acting on the underground structure from ground. Secondly, 1/4 scaled loading tests were conducted, with reproducing complex 3D loading conditions of fault displacement against the box-shaped RC underground structure. Non-linear responses, such as cracking or bar yielding, of the structure were measured. 3D FEM simulations were also conducted targeting on the loading test results. After these code validations, soil-structure coupled analysis were conducted with parameter of overburden of 1m, 8m and 25m as impact assessments of the fault displacement against a supposed actual scale underground RC structure.

Followings are outcomes. (a) Earth pressure calculated by 2D FEM with Drucker-Prager model is good agreement with experimental result up to the fault displacement of 0.5m. (b) Comparing on simulation results and loading test results, the reproducibility of the 3D FEM code on complex nonlinear responses and failure mode of the RC underground structure were verified. (c) Basing on the impact assessment results, collapse of the underground structure never occur for the cases with shallow overburden because of yielding of earth pressure occurred ahead of occurrence of bending yield of structures. (d) In the case with a deep overburden, shear failure occurred on the middle wall, which resulted in the structure being destroyed in advance.

*Keywords: Fault displacement, RC underground structure, Centrifuge, Loading test, Nonlinear 3D FEM*

### 1. Introduction

After the 2011 off the Pacific coast of Tohoku Earthquake, the safety verification for critical facilities of lifeline systems such as nuclear power plants are required not only for earthquake ground motion and tsunami but also for various earthquake related events. The fault displacement is one of the events for which safety verification is required. There are only a few reports about the damage of the underground structure, which were constructed on the bedrock, by the fault displacement; deformation due to the fault displacement occurred in the lining concrete of bullet train (Shinkansen) tunnel during the 2004 Niigata Chuetsu Earthquake [1] and road tunnels during the 2016 Kumamoto Earthquake [2]. Generally, such damage will occur in linear structures such as tunnels, since for these structures the fault line cannot be avoided, and they will intersect with it due to their shapes.

When a vertical displacement occurs on the fault under an underground structure, it suffers complex three-dimensional damage depending on location and angle of fault, and interaction between surrounding ground and the structure. The box culvert, chosen as a target underground structure in this study, is a high-order statically indeterminate structure composed of multiple members. Since the load acting on the fault is due to the ground displacement, not only the force capacity against soil pressure but also the ductility capacity with the redistribution of the stress after the maximum strength is an important performance. It is necessary to evaluate up to the strain level that greatly exceeds the yield for the required performance such as the water flow function. However, the deformation performance up to the strain level that greatly exceeds the yield has generally been studied in the transverse direction (perpendicular to the axis) of the box culvert, mainly for behavior during earthquakes. Thus, it has not been sufficiently studied the complicated three-



dimensional deformation and its damage mode of the box culverts subjected to the ground displacement of the fault crossing the axis of the box culvert.

Aim of this study is to evaluate the impact of the fault displacements against the RC box culvert. Series of experimental studies and numerical simulations were conducted.

Firstly, centrifuge experiments were conducted to investigate the characteristics of soil pressure acting on the underground structure quantitatively during the fault movement. Numerical simulations, utilizing a Nonlinear 3D FEM code named FINAL-GEO, were conducted to investigate the reproducibility of the external force acting on the underground structure.

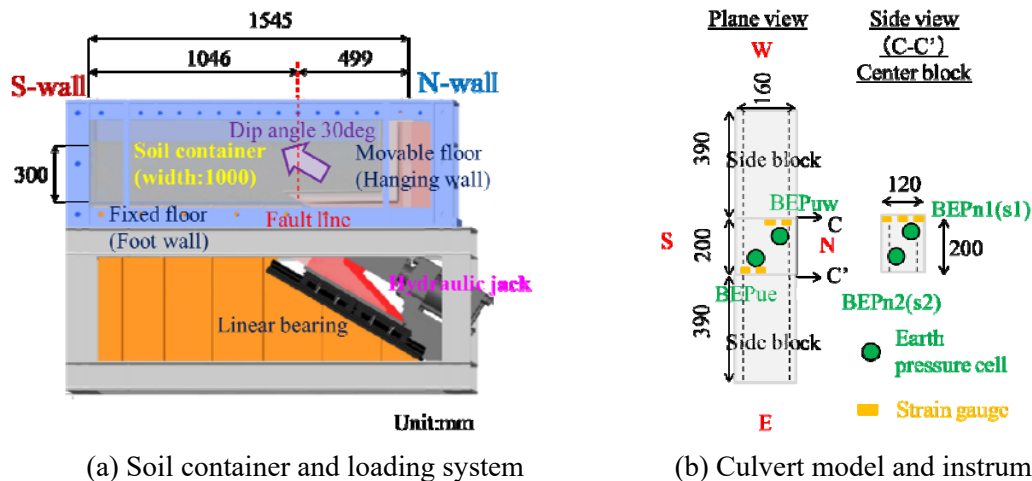
Secondly, 1/4 scaled loading tests were conducted, with reproducing complex 3D loading conditions of fault displacement against the RC box culvert. Non-linear responses, such as cracking or bar yielding of the structure were measured utilizing new measurement devices including optical/image sensors. Then, 3D FEM simulations, utilizing FINAL, were conducted to investigate the reproducibility of complex nonlinear responses and failure mode of the RC underground structure.

After the code validation of Nonlinear 3D FEM code, FINAL/FINAL-GEO, in terms of both soil action and structure response, impact assessments of the fault displacement against a supposed actual scale underground RC structures were conducted based on numerical simulation using FINAL-GEO.

## 2. Centrifuge Experiment[3]

### 2.1 Specimen, soil container and loading setup

To investigate the characteristics of soil pressure acting on the underground structure quantitatively during the fault movement, a soil container with loading jack to reproduce the reverse fault displacement as shown in Figure 1 was constructed and 1/50 scaled centrifuge experiments were conducted. This soil container had a floor fixed directly to the experimental frame and a movable floor connecting to the hydraulic jack to raise at 30 degrees from the horizontal plane. In the centrifuge experiment, model scale was 1/50 and centrifugal gravity was 50g.



(a) Soil container and loading system

(b) Culvert model and instrumentation

Figure 1 Outline of centrifuge experiment for reverse fault rupture

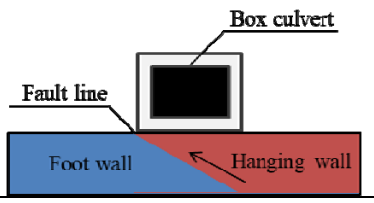
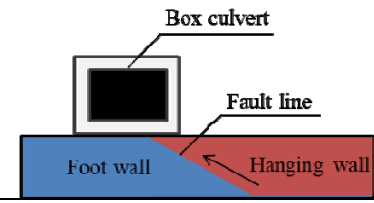
The ground material was dry Gifu quartz sand No. 7 ( $D_{50}=0.1\text{mm}$ ), and a model ground with an equivalent ground thickness of 15m was created by compacting with vibrations with a target relative density of 90%. The model of the underground structure was an RC box culvert structure with a physical size of 8m x 6m, a floor slab and a side wall thickness of 1.4m in prototype, and it was made by cutting an aluminum block so that the cross-sectional stiffness ( $EI$ ) became equivalent to the prototype structure.

In this experiment, the transverse direction of the structure was evaluated. Thus, the culvert model was installed along the fault strike direction. The culvert model was divided into three parts with the length of 395mm, 200mm and 395mm, respectively, and the instrumentation was set to the center.



As shown in Table 1, three experimental cases were conducted; only the ground without the structure were constructed (case 1), a whole part of the culvert model were set on the movable floor (case 2) and the fault line position was directly below the structure (1/4 from the right edge) (case 3). In this paper represents the results of cases 1 and 2 due to limitation of space.

Table 1 Cases of experiments and model conditions

Case	Ground condition	Box culvert model	Max. fault displacement	Culvert location
1		-		-
2	Dry sand (Gifu sand) Depth:300mm (15m in proto type)	Height:120mm (6m) Width:160mm (8m) Length of center block: 200mm (10m) Wall thickness: 20mm (1m)	$\delta_{\max}=100\text{mm}$ (5m)	
3	Unit weight: 15kN/m <sup>3</sup> (Dr=90%)	Covered soil thickness: 180mm (9m)	$\delta_{\max}=60\text{mm}$ (3m)	

In the experiment, at first, centrifugal gravity with 50g was loaded. Then fault displacement was applied to the model ground. Because the dry sand was used to the model ground, the effect of the loading speed was assumed to be negligible. Thus, the fault displacement was loaded stepwise, and deformation of the ground was checked in each step.

## 2.2 Ground deformation

Photo 1 shows deformed ground in case 2. The ground on the movable floor (N wall side) was raised and shear band was generated and reached to the ground surface. The direction of the shear band corresponded to the displacement direction of the fault. Figure 2 shows the ground surface displacement. The ground surface deformation in the case 2 was almost similar to that of case 1.

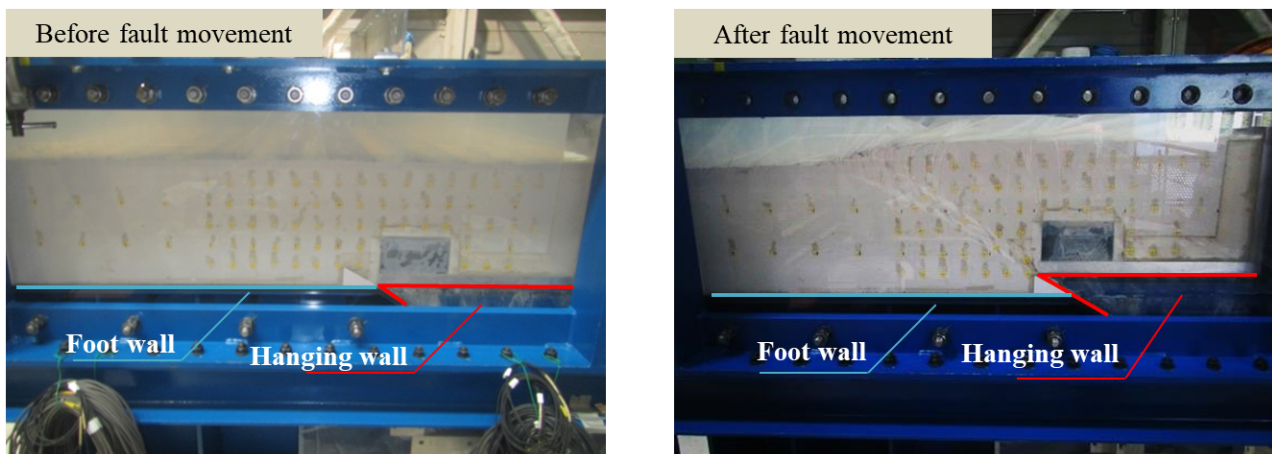


Photo 1 Comparison of ground shapes (case 2)

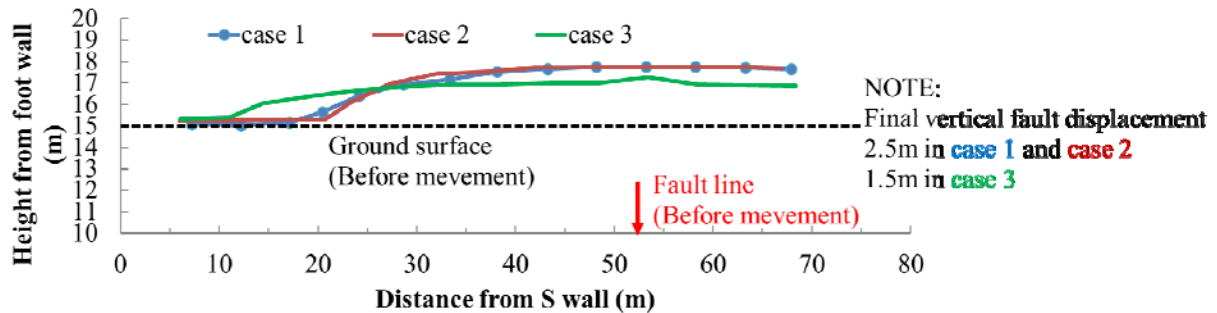


Figure 2 Comparison of ground surface deformations after fault movement

### 2.3 Soil pressure

To evaluate the external soil pressure, pressure cells were installed on top slab and both (N and S) side walls. Because of limitation of space, relations between external force induced by soil reaction vs. fault displacement will be shown in Figure 4 later, together with simulated results as comparison. Note that the external force is calculated by multiplying the measured soil pressure by the area of the surface on which the pressure cells were installed.

It can be seen that the external force acting on the top slab was constant at the initial soil pressure regardless of the installation position of the culvert model and the amount of the fault displacement. On the other hand, the external force acting to the side wall increased when the fault displacement increased. In the case 2, the external force on the S side wall reached a peak at 0.5m fault displacement and then gradually rises to a maximum value of 55MN at 3m fault displacement. On the N side wall, the external force gradually increased from the initial state and reached a maximum value of 45MN.

### 2.4 Analytical simulation

Nonlinear FEM analysis was conducted to reproduce the characteristics of the external force acting on the top slab and the side walls described above. Large scale nonlinear FEM analysis program named FINAL-GEO was used for verification of soil pressure reproduction. Figure 3 shows 2D FEM model. Both soil and structure are idealized as quadrilateral elements with size 0.5m in horizontal by 0.25m in vertical. The fixed and movable floors are assumed to be rigid and the fixed floor is idealized using fixed boundary conditions and the movable floor imposes the fault displacement. Joint elements are installed between structure, ground and container to reproduce the behavior of sliding and uplift of the structure. Nonlinear behavior of the ground material is idealized using the Drucker-Prager model [4] and the culvert model was idealized as the linear elastic. Parameters for the Drucker-Prager model are decided based on the consolidated drain tri-axial test of the soil material as shown in Table 2 and pressure dependent modulus of deformation is also considered. Although case 1 and case 2 were chosen as a simulation target, results from case 2 will be discussed in this paper due to limitation of pages.

Figure 4 shows the calculated ground deformation shape at the fault displacement of  $\delta=0.5\text{m}$  as (a), and external force transitions acting on the top slab and the side walls as (b) through (d). The measured values are also shown as dashed line for comparison. As shown in Figure 5, the relationship between the fault displacement and the external force can reproduce the experimental results until the fault displacement reaches at about 0.5m, at which the ground surface deformation shape matched as (a). On the other hand, in the experiment, the external force yielded at the fault displacement of 0.5m, then gradually increased and reached the maximum value at the fault displacement of 3m, while the external force continuously increases and reaches twice the experimental results in the analysis. Note that the reproductivity of the strain distribution of culvert is also verified by the analysis through the fault displacement of  $\delta=0.5\text{m}$ .

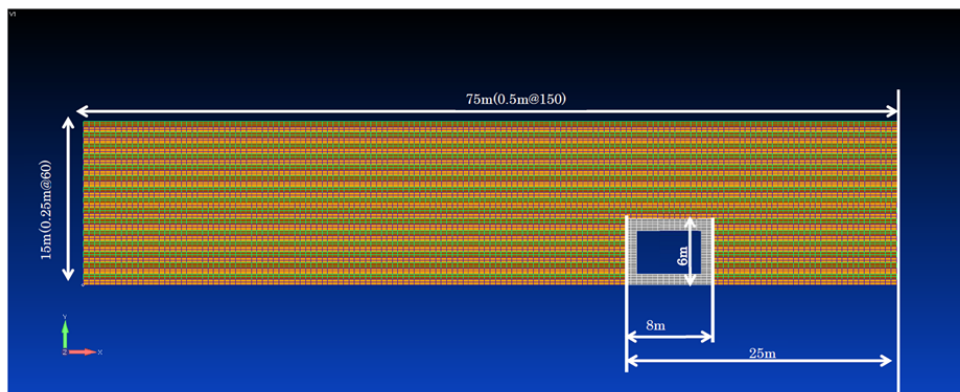


Figure 3 2D-FE model for centrifuge fault simulation (case 2)

Table 2 Parameters of soil model (Drucker-Prager model)

Unit weight (kN/m <sup>3</sup> )	Deformation coefficient $E_s$ (MN/m <sup>2</sup> )	Friction angle $\phi$ (deg)	Cohesion $c$ (kN/m <sup>2</sup> )	Poisson's ratio $\nu$
15.0	23,000	38	1.0	0.33

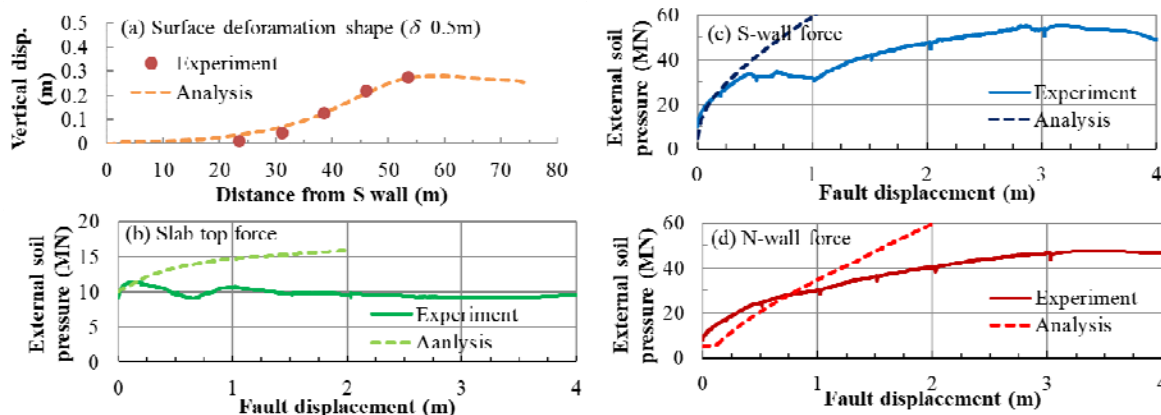


Figure 4 Comparison of measured and calculated ground deformation shape and external force transitions acting on the culvert (case 2)

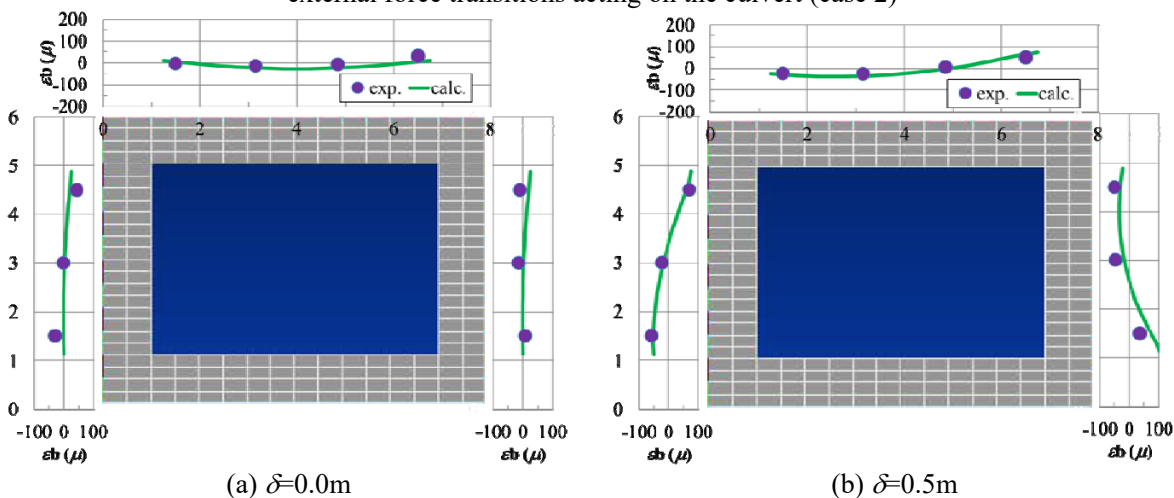


Figure 5 Comparison of measured and calculated bending strain distributions on top slab and side walls of the culvert (case 2)



Figure 5 shows comparison of the measured and calculated bending strain distributions on top slab and side walls at the fault displacement of  $\delta=0.0\text{m}$  and  $0.5\text{m}$ , respectively. In the bending strain distribution of the side wall, deformation mode from  $\delta=0.0\text{m}$  through  $0.5\text{m}$  is reproduced in terms of both inward fluctuation at the center of the span of each wall member, and quantitatively. In terms of axial strain, which could not be presented on this paper due to space limitation, it was seen that the axial strain on the side wall does not fluctuate with increase of fault displacement and remains almost constant in both experiment and analysis results, because of the vertical external force acting on the top slab has not been affected by the fault movement.

### 3. Loading experiment [5]

#### 3.1 Specimen and loading setup

To investigate the complex damage process subjected complex three-dimensional deformations due to the fault displacement, a loading experiment was conducted using 1/4 scaled RC box culvert specimen as shown in Figure 6.

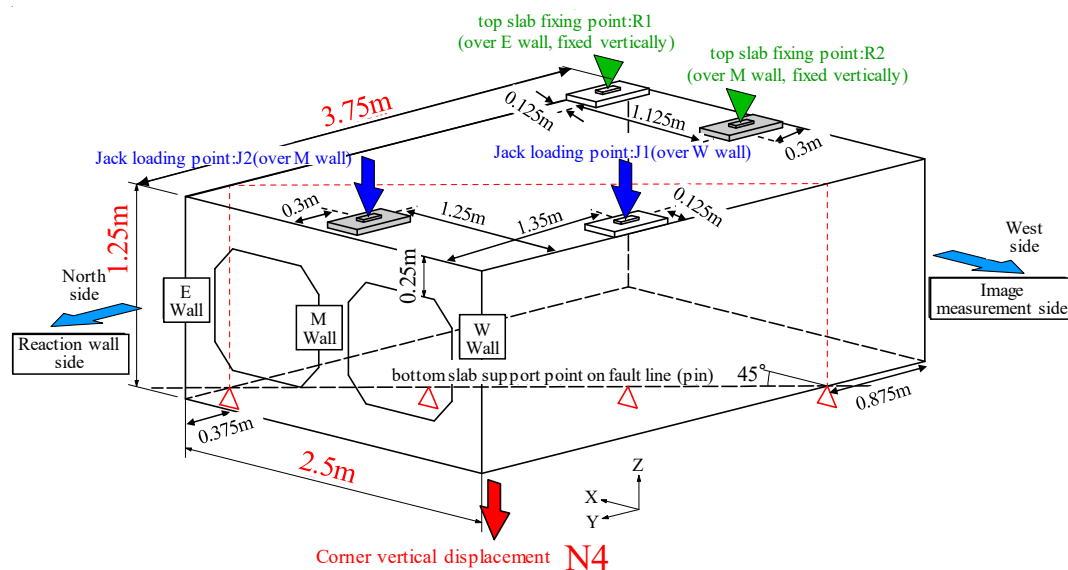


Figure 6 RC box culvert specimen and loading setup

A double cell box culvert model is supported by a linear bearing, which simulates a fault line oblique to the structure axis at 45 degrees. Hence, support condition of a structure supported by bedrock at the time of a dip-slip displacement is simulated. In addition, the overburden load acting on the top slab of the structure is simulated by two jacks and two fixed point reaction forces. The loading is performed until the corner vertical displacement shown in Figure 6 reached 140mm.

To measure the complex deformation of the specimen, not only conventional instrumentation such as displacement transducers and strain gauges but also the image processing measurement were used.

#### 3.2 Relationship between load and displacement and damage process

In the experiment, loading was performed up to 140 mm at the monitoring displacement at the corner of the bottom slab where displacement was largest. Figure 7 shows jack load vs. monitoring displacement relation. Cracks occurred at a monitoring displacement of 5.9 mm, and the reinforcement in the top slab yielded at about 20 mm. After occurrence of the top slab yield, little load increment was seen with deformation



progress of the structure. At a monitoring displacement of 140 mm, crack width became over 20 mm, and the strain of the upper transverse reinforcement was 5-8%. Therefore, the minimum required performance was confirmed as maintaining the inner space of waterways because no brittle failure occurred even though a lot of large cracks developed on the specimen. However, since large crack development as its width of 20 mm, a further study on the performance evaluation of water leakage in the RC structures with large cracks is required in the future. The loading was stopped at 140 mm of monitoring displacement due to the limitation of the jack stroke. Figure 8 shows crack distributions of the specimen after loading experiment.

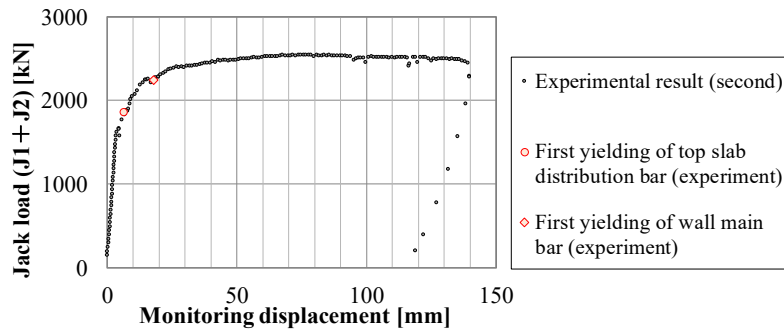


Figure 7 Jack load vs. monitoring displacement relationship



(a) Top slab



(b) W side wall

Figure 8 Cracks of the specimen after the loading experiment

On the top slab, cracks are widely distributed, but cracks with large width concentrated around the fault line. It is seen that cracks developed in diagonal direction against the structure axis, pointing the direction of the bearing line (45 degrees), but slightly inclined in the transverse direction. That cause could be due to torsion and moment-shift produced by the movement of the location of loading and supporting point.

The cracks on the side wall are more concentrated than the top plate. Especially on the west side wall, it is concentrated between the bearing position and the position of the loading jack. Thus, these cracks are bending shear cracks.

### 3.4 Strain distribution

Figure 9 shows maximum principal strain distribution obtained by image processing devices based on the digital image correlation method[6]. Note that the pin bearing and the loading jack were set at the lower right and the upper left of the measurement range, respectively.

At a monitoring displacement of 5.9 mm, a large strain of more than 2% was obtained at the crack position at the same time as the crack appeared on the side wall. Because the obtained strain is defined as the average strain in a finite area including the crack, which is a discontinuous point, large strain was obtained even at the small global deformation of the specimen. Then, as the monitoring displacement increased, the number of cracks increased, as well as increase of the strain at the cracks with the opening of the cracks.



After the monitoring displacement reached 40.0mm, increase of number of cracks stopped while developing the crack strain larger, because of cracks previously occurred became wider in its width.

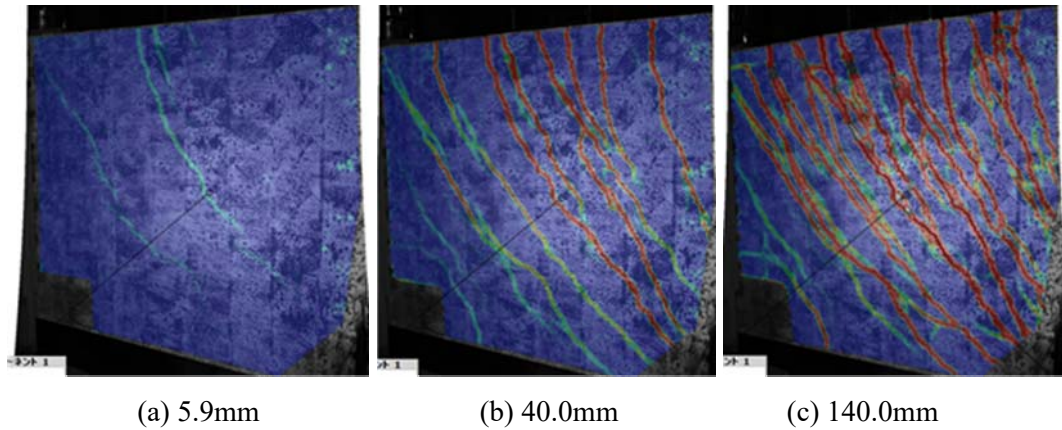


Figure 9 Maximum principal strain distribution

### 3.5 Analytical simulation

Analytical simulation of the loading experiment is conducted. The concrete members with distributed reinforcement are idealized as hexahedron elements with embedded reinforcements and main reinforcement is idealized as truss elements. Smearred crack model including non-orthogonal multidirectional cracks is used as constitutive law of concrete. Modified Ahmad model [7] and Nakamura-Higai model [8] are used as characteristics of compression hysteresis before and after peak, respectively. Failure criterion of the concrete is assumed to be Ottosen's four parameter model with parameters proposed by Hatanaka et al [7]. Tension stiffening and shear transfer characteristics also consider by Izumo et al. model [9] and Naganuma model [10], respectively. Bilinear hysteresis model is used as constitutive law of reinforcements.

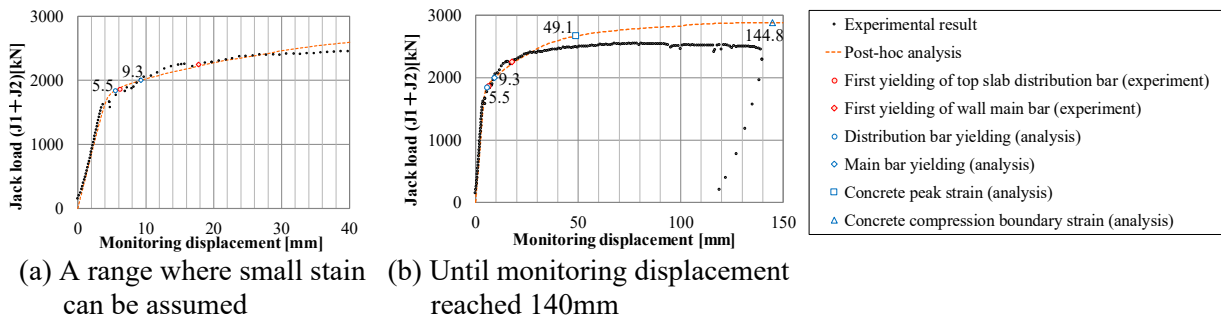


Figure 10 P~δ relationship for test and analysis

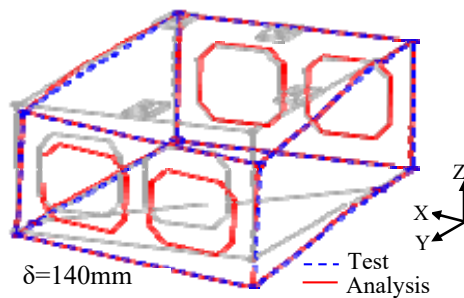


Figure 11 Deformation of the specimen at monitoring displacement of 140 mm



Figure 10 shows jack load vs. the monitoring displacement relation. In Figure 10, experimental results also shown for comparison. Note that the applicable strain range of the constitutive law described above is small strain, which corresponds to a range where the monitoring displacement is up to 40mm. Therefore, Figure 10(a) shows the enlarged graph with a range of the monitoring displacement up to 40 mm. Initial yield of the distribution reinforcement at top slab occurred at the monitoring displacement of 5mm, and the jack load remained almost the same from the monitoring displacement of 30mm up to that of 140mm. The point of initial yield of top slab reinforcement in the analysis is consistent with the loading test. In addition, the P- $\delta$  relationship well reproduces the experimental results up to the monitoring displacement of 40 mm, corresponding to 8 times of the yield displacement that is considered as a usual design target range. If the displacement is larger than that value, the load obtained by analysis tends to overestimate the experimental value slightly, but it shows a stable transition as in the experiment. Furthermore, since the final deformation mode of experiment is in good agreement with the analysis result as shown in Figure 11, it is considered that the damage mode, which conceivable as the bending of the whole structure under the top slab side in tension and the bottom slab side in compression with taking the fault line as central point, can be accurately reproduced even the monitoring displacement exceeds 40 mm.

#### 4. Soil-Structure Coupled Analysis

To investigate the complex damage mode of a RC box culvert subjected to the fault displacement, 3D nonlinear analysis is conducted based on the analytical idealization verified in the above sections. The three-dimensional analysis model and reinforcement details of the target structure are given in Figures 12 and 13. Dimensions of the ground model has 140m in length, 120m in width, and maximum 50m in depth (depends on cover soil depth). A double cell RC box culvert model, 12m in width, 9m in height and 15m in length is placed on the fault line by 45 degree in diagonal to the structural axis. Fault dip angle is 80 degree.

The analysis was performed by FINAL-GEO. The bedrock, ground and concrete part of the structure are modeled as hexahedral elements. Reinforcements are modeled with truss elements only for the haunch, and the rest reinforcements are idealized as the embedded reinforcements. The bedrock is idealized as an elastic body and ground above the bedrock, concrete and the reinforcements are idealized using the material constitutive laws verified in the above sections. Joint elements were installed between structure, ground and bedrock to consider the interaction such as contact, spalling and friction, of these members.

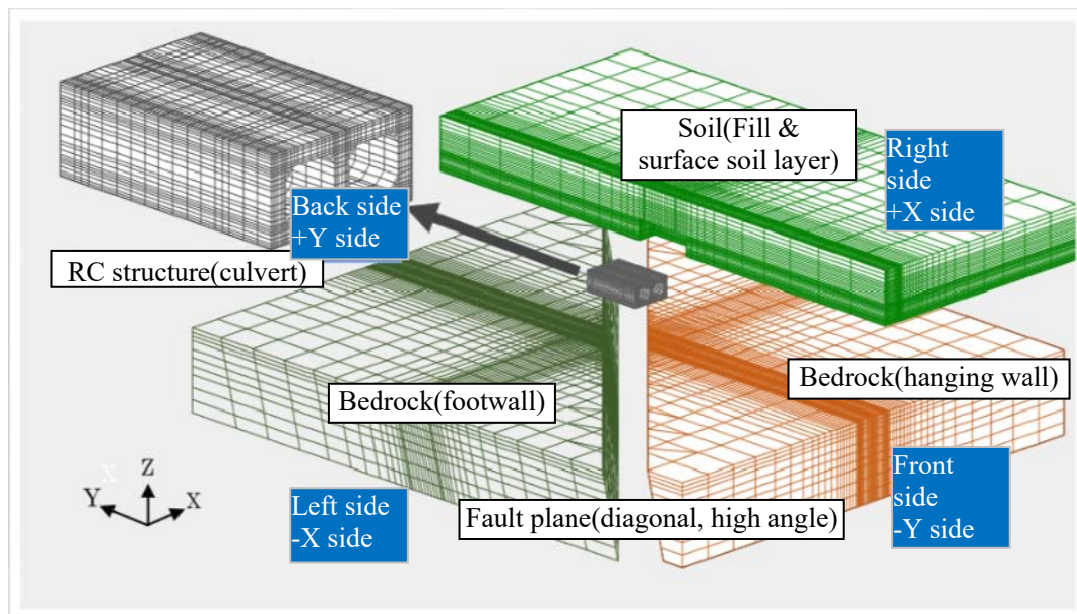


Figure 12 3D Analysis model

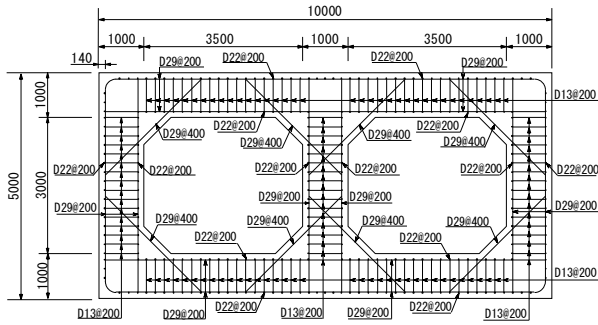


Figure 13 Target structure

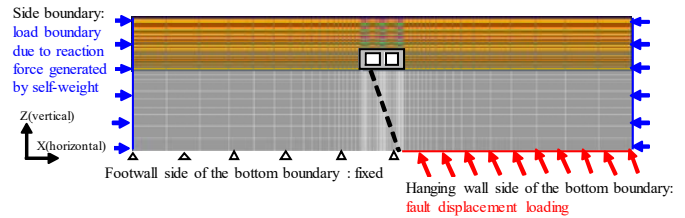


Figure 14 Boundary conditions during fault displacement loading

Table 1 Comparison of strain contours of structures and ground

Contour	C-1.1 Overburden 1m (Fault displacement 100mm)	C-1.2 Overburden 8m (Fault displacement 500mm)	C-1.3 Overburden 25m (Fault displacement 200mm)
Rebar strain on structure axis direction			
Concrete Principal compression strain (bottom slab)			
Concrete Principal compression strain (wall/lower haunch cross-section)			
Ground Maximum shear strain (Distribution in the cross section passing through the center of the structure)			

The forced displacement analysis, which imitate the fault displacement load, was conducted after the self-weight analysis. At the self-weight analysis, boundary condition was set as vertical rollers for each side and a fixed boundary for the bottom of the model. During the forced displacement analysis, stress boundary was applied to each side of the model which is subjected the horizontal reaction force generated by self-weight of soil. Then, forced displacement analysis was performed by applying displacement on the hanging wall side of the bottom of bedrock with the footwall side being fixed (Figure 14).



In this study, three analytical cases are conducted with different overburden above the structure of 1m, 8m and 25m. Typical reinforcement and concrete compression strain contours indicating damage and failure of the structure and maximum shear strain contour indicating ground failure status for each case with different overburden of 1m, 8m, 25m are shown in Table 7.

In the case of 1m overburden at 100mm fault displacement, the region where the maximum shear strain exceeds 2% spreads from upper left corner of the structure through the ground surface as observed from the maximum shear strain contour of the ground. Although the perfect elast-plastic Drucker-Prager model is used as the constitutive law of the ground element, the clear ground failure can not be seen. Almost no damage on the structure has been observed at this point.

In the case of 8m overburden at 500mm fault displacement, yielding of axial rebars of the structure is observed at the whole area of the top slab, and maximum  $4,000\mu$  of compressive strain occurs along the fault line under the bottom slab. Hence, progress of damage due to overall bending of the structure, of which the top slab side is under tension and bottom slab side is under compression, can be confirmed. However, the concrete compression strain of  $10,000\mu$ , which is regarded as the limit state of failure defined in the design specifications of the nuclear power plant, has not been observed. In terms of the ground, it is observed that the region where the maximum shear strain exceeds 2% spreads from bottom left corner of the structure through the ground surface by the maximum shear strain contour. Although the structure suffered bends and yields, it is considered that the ground collapse may take place before the structural failure.

In the case of 25m overburden, different damage mode is observed compared to that of the case of 8m overburden, even though the overall bending deformation of the structure has occurred in both cases. To clarify this characteristic, the minimum principal strain distribution, which is cut at the lower haunch of the wall member are shown. When the fault displacement has reached 200 mm, a compressive strain over  $10,000\mu$  is occurred in the entire cross-section of the wall which is in the partition behind the fault line. It is considered that after the bending yield of the structure, shear failure is occurred due to shear at the base end of the wall. The increase in the bending resistance of walls by the increase of the compressive axial force growing in the culvert axial direction due to the fault movement. Magnitude of this force depends on the soil thickness, and in the meantime the friction occurred on the top slab, which is proportional to the overburden, considered as the cause of such a failure mode discussed above. Transitions in the cross-section component of the friction force at top slab are shown in Figure 15. It can be easily observed that the generated friction force in the case with 25m overburden is about 3 - 4 times of the case with 8m overburden.

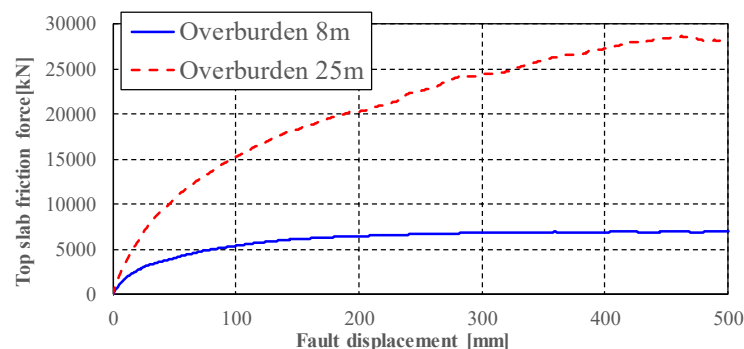


Figure 15 Comparison of the frictional force of the structure top slab

## 5. Conclusions

To evaluate complex damage mode of RC box culvert subjected to the fault displacement, nonlinear FEM analysis modelling and constitutive model of the soil and concrete are verified based on the centrifugal and



loading experiments, and soil-structure coupled analysis is conducted. Based on the experimental and analytical study, the following conclusions may be deduced;

- 1) Based on the centrifugal experiment of a box culvert subjected to the fault displacement, soil pressure acting on the top slab was constant with the initial soil pressure. On the other hand, soil pressure acting on the side walls gradually increased as the fault displacement increased, however, the soil pressure yielded after it reached its peak value.
- 2) Soil pressure calculated using FEM with Drucker-Prager model is good agreement with experimental result up to the fault displacement of 0.5m.
- 3) Based on the loading experiment of a RC box culvert subjected to the fault displacement, complicated damage mode was investigated and FEM analysis modelling and constitutive model of concrete (smeared crack model with non-orthogonal multidirectional cracks) are verified based on the experimental results.
- 4) Soil-structure coupled analysis with the modelling verified based on the experimental results described the above is conducted with parameter of overburden of 1m, 8m and 25m. It is found based on the analytical study that although bending yielding of structures occurred, yielding of ground occurred in advance and the structure did not collapse for the cases with shallow overburden. On the other hand, in the case with a deep overburden, shear failure occurred on the middle wall, which resulted in the structure being destroyed in advance.

## 6. References

- [1] 2004 Niigata-ken Chuetsu Earthquake Emergency Investigation Team in JSCE (2005): Summary of First Investigation of 2004 Niigata-ken Chuetsu Earthquake, JSCE (in Japanese).
- [2] JSCE (2017): Earthquake Damage Inspection Report on 2016 Kumamoto Earthquake, *Series of Earthquake Damage Inspection No. 1*, JSCE (in Japanese).
- [3] Higuchi, S., Kato, I., Sato, S., Itoh, G. and Sato, Y. (2017): Experimental and Numerical Study on the Characteristics of Earth Pressure Acting on the Box-shape Underground Structure Subjected the Strike Slip Fault Displacement, *Journal of JSCE(A1)*, Vol.73, No. 4, pp. I\_19-I\_31 (in Japanese).
- [4] Drucker, D. C. and Prager, W. (1952): Soil Mechanics and Plastic Analysis or Limit Design, *Quarterly of Applied Mathematics*, Vol. 10, pp. 157-165.
- [5] Yamaguchi, K., Itoh, G., Hida, Y., Tanaka, K., Sasaki, T. and Nagai, H. (2020): Loading Test on Box Culvert Subjected to Fault Displacement, *Journal of Structural Engineering*, JSCE, Vol. 66A (in Japanese, in press)
- [6] GOM GmbH (2017): *Digital Image Correlation and Strain Computation Basics*, GOM Testing Technical Documentation.
- [7] Naganuma, K., Yonezawa, K., Kurimoto, O. and Eto, H. (2004): Simulation of Nonlinear Dynamic Response of Reinforced Concrete Scaled Model Using Three Dimensional Finite Element Method, *13th WCEE*, Paper No.586.
- [8] H. Nakamura and T. Higai (1999): Compressive Fracture Energy and Fracture Zone Length of Concrete, *Seminar on Post-peak Behavior of RC Structures Subjected to Seismic Load*, JCI-C51E, Vol.2, pp.259-272.
- [9] J. Izumo, H. Shima and T. Okamura (1987): Analytical Model of Reinforced Concrete Plate Element Subjected to In-plane Internal Force, *Concrete Engineering*, No. 87.9-1, pp. 107-120 (in Japanese).
- [10] Naganuma, K. (1991): Nonlinear Analytical Model for Reinforced Concrete Panels under In-plane Stresses Study on Nonlinear Analytical Method for Reinforced Concrete Wall Structures (Part 1), *Journal of Struct. Constr. Engng*, AIJ, No. 421, pp. 39-48.